

# Solid Splenic Masses: Evaluation with $^{18}\text{F}$ -FDG PET/CT

Ur Metser, MD<sup>1,2</sup>; Elka Miller, MD<sup>2</sup>; Ada Kessler, MD<sup>2</sup>; Hedva Lerman, MD<sup>1</sup>; Gennady Lievshitz, MD<sup>1</sup>; Ran Oren, MD<sup>3</sup>; and Einat Even-Sapir, MD, PhD<sup>1</sup>

<sup>1</sup>Department of Nuclear Medicine, Tel-Aviv Sourasky Medical Center, Sackler Faculty of Medicine, Tel-Aviv University, Tel-Aviv, Israel; <sup>2</sup>Department of Radiology, Tel-Aviv Sourasky Medical Center, Sackler Faculty of Medicine, Tel-Aviv University, Tel-Aviv, Israel; and <sup>3</sup>Department of Gastroenterology, Tel-Aviv Sourasky Medical Center, Sackler Faculty of Medicine, Tel-Aviv University, Tel-Aviv, Israel

Our objective was to assess the role of  $^{18}\text{F}$ -FDG PET/CT in the evaluation of solid splenic masses in patients with a known malignancy and in incidentally found lesions in patients without known malignancy. **Methods:** Two groups of patients were assessed: (a) 68 patients with known malignancy and a focal lesion on PET or a solid mass on CT portions of the PET/CT study; and (b) 20 patients with solid splenic masses on conventional imaging without known malignancy. The standard of reference was histology ( $n = 16$ ) or imaging and clinical follow-up ( $n = 72$ ). The lesion size, the presence of a single versus multiple splenic lesions, and the intensity of  $^{18}\text{F}$ -FDG uptake expressed as a standardized uptake value (SUV) were recorded. The ratio of the SUV in the splenic lesion to the background normal splenic uptake was also calculated. These parameters were compared between benign and malignant lesions within each of the 2 groups of patients and between the 2 groups. **Results:** The sensitivity, specificity, positive predictive value (PPV), and negative predictive value (NPV) of  $^{18}\text{F}$ -FDG PET/CT in differentiating benign from malignant solid splenic lesions in patients with and without malignant disease were 100%, 100%, 100%, and 100% versus 100%, 83%, 80%, and 100%, respectively. In patients with known malignant disease, an SUV threshold of 2.3 correctly differentiated benign from malignant lesions with the sensitivity, specificity, PPV, and NPV of 100%, 100%, 100%, and 100%, respectively. In patients without known malignant disease, false-positive results were due to granulomatous diseases ( $n = 2$ ). **Conclusion:**  $^{18}\text{F}$ -FDG PET can reliably discriminate between benign and malignant solid splenic masses in patients with known  $^{18}\text{F}$ -FDG-avid malignancy. It also appears to have a high NPV in patients with solid splenic masses, without known malignant disease.  $^{18}\text{F}$ -FDG-avid splenic masses in patients without a known malignancy should be further evaluated as, in our series, 80% of them were malignant.

**Key Words:** hematology; oncology; FDG; PET/CT; spleen

**J Nucl Med 2005; 46:52–59**

Received Apr. 19, 2004; revision accepted Jul. 27, 2004.  
For correspondence or reprints contact: Ur Metser, MD, Department of Nuclear Medicine, Tel-Aviv Sourasky Medical Center, 6 Weizman St., Tel-Aviv, 64239 Israel.  
E-mail: [umetser@tasmc.health.gov.il](mailto:umetser@tasmc.health.gov.il)

**A**lthough not as common as focal hepatic masses, solid splenic masses are encountered in routine clinical practice and pose a diagnostic dilemma. Lesions may be discovered incidentally on imaging studies performed for unrelated causes. Malignant solid splenic lesions include lymphoma, leukemic infiltrates, metastases, and, rarely, angiosarcoma (1–5). The most frequently encountered benign solid splenic lesions are hemangiomas, hamartomas, and granulomas (6–8). Rarely, littoral cell angioma, inflammatory pseudotumor, or Gaucher nodules may be seen (9–11).

Almost all imaging modalities have been assessed regarding the identification and characterization of splenic lesions; however, conventional imaging modalities often cannot reliably differentiate benign from malignant lesions (12,13).  $^{18}\text{F}$ -FDG PET is a powerful tool for oncology imaging and is becoming widely available. This functional imaging modality is based on identification of hypermetabolic foci and has been shown to be accurate in staging of lymphoma, lung cancer, melanoma, and gastrointestinal and gynecologic malignancies among other tumors (14–18).

Recently, PET/CT systems, which enable the performance of PET and CT data acquisition at the same setting without changing the patient's positioning, have been introduced in clinical practice (19). Lesions are characterized on the fused PET/CT images by both their metabolic status and their anatomic detail, enabling precise correlation of metabolic activity within a structural abnormality.

The purpose of this study was to assess the role of  $^{18}\text{F}$ -FDG PET/CT in the evaluation of splenic masses in patients with a known malignancy and in incidentally found lesions in patients without a known malignancy. The rationale behind using this imaging modality for characterization of splenic lesions was that malignant diseases most commonly involving the spleen are principally  $^{18}\text{F}$ -FDG-avid diseases, including lymphoma and metastases from malignant melanoma, lung cancer, ovarian cancer, and gastrointestinal malignancies. In contrast, the common benign splenic lesions—that is, hemangiomas and hamartomas—are not expected to show increased  $^{18}\text{F}$ -FDG uptake.

## MATERIALS AND METHODS

### Study Population

The study population included 2 groups of patients. Group A consisted of patients with a known malignancy who had splenic lesions on either the PET or CT portions of the study (a focal increased  $^{18}\text{F}$ -FDG uptake or a solid mass, respectively) (Table 1). Pure cystic lesions and small calcified lesions (the latter presumably representing calcified granulomas) were not included in this study. A retrospective review of our oncology PET/CT scan database for studies performed over an 18-mo period yielded 68 patients (38 men, 30 women; median age, 58.5 y; range, 21–84 y) with known malignant diseases and solid splenic lesions. These patients were sent for staging of a primary malignancy ( $n = 58$ ) or restaging after therapy ( $n = 9$ ). All patients sent for restaging were at least 4 mo after last anticancer systemic therapy. Group B consisted of 20 patients without known malignant disease (13 men, 7 women; median age, 56.5 y; range, 18–89 y) who were sent for  $^{18}\text{F}$ -FDG PET/CT because of a splenic mass on conventional imaging modalities. Data of this group of patients are summarized in Table 2. Our institutional review board does not require their approval and informed consent for review of a patient's records, files, and images.

### Standard of Reference

For group A, a final diagnosis of the splenic lesions was made by splenic biopsy ( $n = 6$ ) or clinical and imaging follow-up ( $n = 62$ ). In group A, an  $^{18}\text{F}$ -FDG-avid lesion was considered true-positive for malignant involvement if proven by biopsy or if resolved after therapy or progressed on follow-up PET/CT or other imaging. An  $^{18}\text{F}$ -FDG-negative CT lesion was considered true-negative if it showed stability in size on conventional imaging follow-up or remained negative on repeated PET/CT.

Histology or clinical and imaging follow-up determined the final diagnosis of splenic lesions also in the 20 patients who did not

have known malignant disease (group B). For  $^{18}\text{F}$ -FDG-avid splenic masses, the final diagnosis was achieved by splenectomy ( $n = 4$ ), splenic biopsy ( $n = 4$ ), or biopsy of a more accessible FDG-avid lesion found on the whole-body PET/CT scan (lymph node,  $n = 1$ ; lung,  $n = 1$ ). It is not practical to histologically confirm all  $^{18}\text{F}$ -FDG-avid lesions. Diagnoses obtained from sites other than the spleen are based on the fact that in routine clinical practice it is assumed that all pathologic sites of uptake are related to a single pathology. Patients with masses that did not show increased uptake of  $^{18}\text{F}$ -FDG had clinical and imaging follow-up (CT,  $n = 8$ ; ultrasound,  $n = 2$ ) (mean, 11 mo; range, 6–17 mo) with stability in the size of the splenic lesion and were free of malignant disease for the follow-up time period.

### PET/CT

Patients were asked to fast for at least 4 h before undergoing the examination. All patients had glucose levels below 150 mg%. The patients received an intravenous injection of 370–666 MBq (10–18 mCi)  $^{18}\text{F}$ -FDG. Data acquisitions were performed within 60–120 min after injection using an integrated in-line PET/CT system (Discovery LS; General Electric Medical Systems). Iodinated oral contrast material was given to opacify loops of bowel on CT.

Data acquisition was as follows: CT was performed first, from the head to the pelvic floor with 140 kV, 80 mA, tube rotation time of 0.5 s, pitch of 6, and 5-mm section thickness, which was matched to PET section thickness. The CT part of the study was performed using a shallow breathing technique. Immediately after CT, a PET emission scan was obtained that covered the identical transverse field of view. The acquisition time was 5 min per each table position. PET image datasets were reconstructed iteratively by using CT data for attenuation correction, and coregistered images were displayed on a workstation (Xeleris; Elgems).

### Data Analysis and Statistics

Studies of all patients in both study groups were retrieved and read in consensus by a panel of 2 experts. The panel recorded the largest diameter of the splenic masses, presence of a single mass versus multiple lesions within the spleen, and avidity of the splenic mass to  $^{18}\text{F}$ -FDG, visually and by obtaining standardized uptake value (SUV Lesion [SUV L]) measurements. On visual inspection, a lesion was considered as showing pathologically increased uptake if its uptake was higher than the physiologic uptake of the surrounding splenic parenchyma. A region of interest was drawn with a diameter of two thirds of the diameter of the lesion to minimize partial-volume effects. In cases in which a splenic lesion was identified on CT without increased  $^{18}\text{F}$ -FDG uptake, the SUV was measured based on the location of the lesion on coregistered images. The outline of the spleen was examined on coregistered images to confirm adequate image registration. In studies with  $>1$  splenic mass, the largest and smallest lesions were analyzed. The SUV of the normal spleen was also measured with a similar-sized region of interest, at a location distant from the focal splenic lesion (SUV Background [SUV B]). To eliminate the possible effect of variability in the normal splenic  $^{18}\text{F}$ -FDG uptake of  $^{18}\text{F}$ -FDG among different individuals, the ratio between SUV L and SUV B was calculated. In addition, additional pathologic  $^{18}\text{F}$ -FDG-avid foci on the whole-body  $^{18}\text{F}$ -FDG PET/CT study were noted.

The SAS system for Windows, version 8.01, was used for statistical analysis. Comparison of SUVs in malignant and benign lesions (SUV L), SUVs of normal background splenic uptake of  $^{18}\text{F}$ -FDG (SUV B), and ratios of SUV L to SUV B was performed

**TABLE 1**

Primary Malignancies in Oncologic Patients (Group A) in Whom Splenic Lesions Were Suggested on PET/CT

Primary malignancy	No. of patients with $^{18}\text{F}$ -FDG-avid splenic lesion* ( $n = 60$ )	No. of patients with non- $^{18}\text{F}$ -FDG-avid splenic lesion† ( $n = 8$ )
Lymphoma	34*	3
Melanoma	6	1
Lung cancer	6	2
Colon cancer	5*	
Ovarian cancer	4	
Squamous cell carcinoma	2	1
Breast cancer	1	
Esophageal cancer	1	
Adenocarcinoma of unknown primary	1	
Papillary thyroid cancer	1	
Seminoma		1

\*Single patient with 2 known primary malignancies.

†Lesions refer to hypodense solid lesions on CT data of study with no increased  $^{18}\text{F}$ -FDG uptake.

TABLE 2

Clinical Data, <sup>18</sup>F-FDG Avidity, and Final Diagnosis of Splenic Lesions in Patients Without Known Malignancy (Group B)

Patient no.	Age (y)	Sex	Clinical indication	<sup>18</sup> F-FDG avidity	Method of diagnosis	Final diagnosis
1	89	M	Abdominal pain; CT lesion	+	SPL FNA	Gastric cancer
2	18	F	Abdominal pain; CT lesion	+	Surgery	Brucellosis
3	52	M	Abdominal pain; CT lesions	+	LN Bx	Lymphoma
4	66	M	Incidental US finding	+	SPL FNA	Lymphoma
5	55	F	Incidental CT finding	+	Lung Bx	Sarcoidosis
6	65	M	Incidental CT finding	+	SPL FNA	Lymphoma
7	69	F	Incidental CT finding; previous malaria	+	Surgery	Lymphoma
8	40	F	Incidental US finding	+	Surgery	Lymphoma
9	66	M	Incidental CT finding	+	SPL FNA	Lymphoma
10	59	M	Abdominal pain; CT lesions	+	Surgery	Lymphoma
11	62	F	Incidental CT finding	–	C and I F/U	NED
12	33	M	Incidental US finding	–	C and I F/U	NED
13	53	M	Incidental US finding	–	C and I F/U	NED
14	55	M	Incidental CT finding	–	C and I F/U	NED
15	48	F	Incidental US finding	–	C and I F/U	NED
16	58	M	Incidental US finding	–	C and I F/U	NED
17	48	M	Incidental CT finding	–	C and I F/U	NED
18	59	F	Incidental US finding	–	C and I F/U	NED
19	62	M	Incidental CT finding	–	C and I F/U	NED
20	65	M	Incidental US finding	–	C and I F/U	NED

SPL = spleen; FNA = fine-needle aspiration; LN = lymph node; Bx = biopsy; US = ultrasound; C and I F/U = clinical and imaging follow-up; NED = no evidence of malignant disease on imaging work-up and stability of lesion on follow-up imaging.

for patients with benign and malignant splenic lesions within each of the 2 groups of patients and between the 2 groups. The Student *t* test was used and  $P < 0.05$  was considered statistically significant. Receiver operating characteristic (ROC) curve analysis determined the most suitable SUV threshold and the SUV L-to-SUV B ratio to differentiate benign and malignant splenic lesions in both groups of patients. For patients with  $>1$  splenic lesion, the correlation coefficient was calculated for the correlation between lesion size and SUV measurements.

## RESULTS

Table 3 summarizes the results for the 2 groups of patients according to the number of splenic lesions identified. The multiplicity of lesions in the spleen (regardless of <sup>18</sup>F-FDG uptake) had a positive predictive value (PPV) of 81.5%. However, solitary splenic lesions (regardless of <sup>18</sup>F-FDG uptake) were malignant in 81.7% of cases.

TABLE 3

Distribution of Splenic Lesions Based on Number of Lesions in Spleen and Type of Lesion in Both Groups of Patients

Splenic lesions	Malignant		Benign	
	Group A	Group B	Group A	Group B
Single	42	4	7	4
Multiple	18	4	1	4

Twenty-seven patients in group A had nonlymphomatous malignancy and malignant splenic involvement. In 23 of them (23/27, 85.2%), the splenic metastases were in addition to widespread metastatic disease (Fig. 1); 1 patient with melanoma had metastatic disease limited to the spleen, and 3 patients (melanoma,  $n = 1$ ; ovarian cancer,  $n = 1$ ; squamous cell carcinoma of the anus,  $n = 1$ ) had only 1 metastasis in addition to the spleen. This additional tumor site was located in a lymph node or the peritoneum. The mean size of malignant splenic lesions was 1.7 cm (range, 0.5–15.6 cm).

The mean SUV L of all benign lesions was  $1.87 \pm 0.32$  (minimum value, 1.17; maximal value, 2.1; variation coefficient, 17.19; 95% confidence interval, 1.6–2.13). The mean SUV L of all malignant lesions was  $7.86 \pm 5.57$  (minimum value, 2.42; maximal value, 29.6; variation coefficient, 70.85; 95% confidence interval, 6.59–9.12). Ratios of the mean SUV L of benign splenic lesions to the SUV B were  $1.04 \pm 0.21$  (minimum value, 0.63; maximal value, 1.24; variation coefficient, 19.91; 95% confidence interval, 0.87–1.21). Ratios of the mean SUV L of malignant splenic lesions to the SUV B were  $3.91 \pm 2.78$  (minimum value, 1.23; maximal value, 14.03; variation coefficient, 71.11; 95% confidence interval, 3.28–4.45). Differences in SUV L and in the SUV L-to-SUV B ratios between benign and malignant groups were statistically significant ( $P < 0.01$  and  $P < 0.01$ , respectively). In the group of patients with

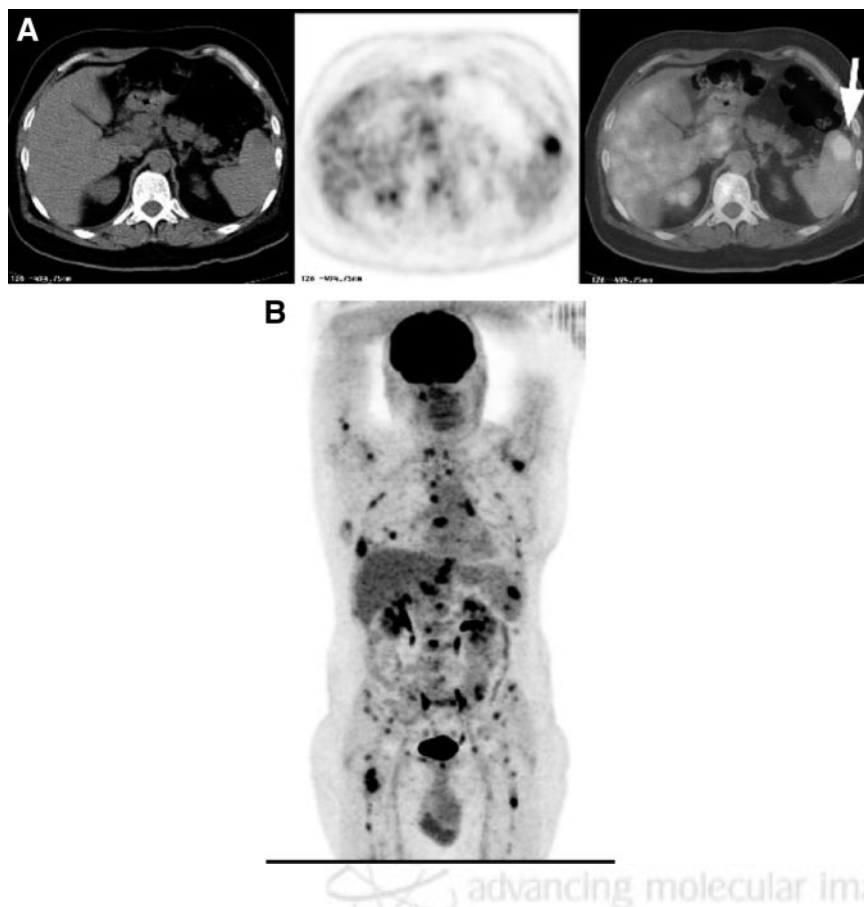


**FIGURE 1.** Solitary splenic metastasis in presence of disseminated metastatic disease: 62-y-old man with lung cancer. (A) Axial PET/CT images show  $^{18}\text{F}$ -FDG-avid metastatic deposit in anterior aspect of spleen (arrow). Follow-up contrast-enhanced CT showed progression of splenic mass (not shown). (B) Maximum-intensity-projection PET image shows disseminated metastatic disease in bone, liver, lymph nodes, and spleen.

splenic mass and known malignant disease, the sensitivity, specificity, PPV, and negative predictive value (NPV) of visual analysis of  $^{18}\text{F}$ -FDG PET/CT in differentiating benign from malignant solid splenic lesions were 100%, 100%, 100%, and 100%, respectively. Using ROC curve analysis, the best SUV threshold for 100% NPV, with the highest possible PPV, was 2.3 (with a sensitivity, specificity, accuracy, PPV, and NPV of 100%, 100%, 100%, 100%, and 100%, respectively) and the best ratio threshold was 1.2 (with a sensitivity, specificity, accuracy, PPV, and NPV of 100%, 75%, 98%, 97%, and 100%, respectively).

Of the 20 patients referred for evaluation of a splenic mass without a previously diagnosed malignancy, 10 patients (50%) had abnormal uptake of  $^{18}\text{F}$ -FDG in a splenic lesion. Of these 10 patients, 2 had inflammatory lesions (sarcoidosis,  $n = 1$ ; brucellosis,  $n = 1$ ) and 8 patients had malignant disease (lymphoma,  $n = 7$ ; metastatic deposit from gastric cancer,  $n = 1$ ). Five of the 7 (71.4%) patients with lymphoma had additional  $^{18}\text{F}$ -FDG-avid disease in lymph nodes, whereas 2 patients had lymphoma limited to the spleen, consistent with primary splenic lymphoma (Fig. 2). The mean size of splenic lesions was 2.05 cm (range, 0.5–12.5 cm). Of these 20 patients (with 29 splenic lesions analyzed), 9 (45%) had  $\geq 2$  lesions in the spleen. The mean SUV of all benign lesions was  $2.29 \pm 1.36$  (minimum value, 0.63; maximal value, 6.30; variation coefficient, 59.30; 95% confidence interval, 1.62–2.96). The mean SUV

of all malignant lesions was  $9.11 \pm 6.95$  (minimum value, 2.3; maximal value, 26.6; variation coefficient, 76.25; 95% confidence interval, 4.74–13.49). In this group of patients, ratios of the mean SUV L to SUV B in benign splenic lesions were  $1.49 \pm 1.06$  (minimum value, 0.34; maximal value, 4.5; variation coefficient, 70.68; 95% confidence interval, 0.53–1.58). Ratios of the mean SUV L to SUV B in malignant splenic lesions were  $4.48 \pm 3.02$  (minimum value, 1.51; maximal value, 11.57; variation coefficient, 65.56; 95% confidence interval, 2.45–6.51). Differences in SUV L and in SUV L-to-SUV B ratios between benign and malignant groups were statistically significant ( $P < 0.005$  and  $P < 0.005$ , respectively). In the group of patients without known malignant disease, the sensitivity, specificity, PPV, and NPV of visual analysis of  $^{18}\text{F}$ -FDG PET/CT in differentiating benign from malignant solid splenic lesions was 100%, 83%, 80%, and 100%, respectively. Using ROC curve analysis, the best SUV threshold for 100% NPV, with highest possible PPV, was 2.2 (with sensitivity, specificity, accuracy, PPV, and NPV of 100%, 71%, 83%, 71%, and 100%, respectively) and a ratio threshold of 1.5 (with sensitivity, specificity, accuracy, PPV, and NPV of 100%, 76%, 86%, 75%, and 100%, respectively).

No statistically significant difference was noted between SUV B of patients with malignant lesions in both groups of patients (with and without known malignancy) or between SUV B of patients with malignant splenic lesions and be-

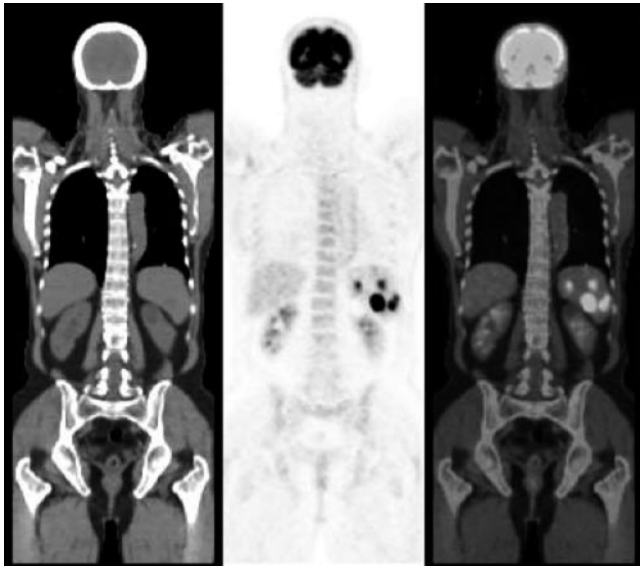


**FIGURE 2.** Primary splenic lymphoma: 66-y-old man without previously diagnosed malignancy. Coronal PET/CT images show multiple  $^{18}\text{F}$ -FDG-avid splenic masses, proven to be non-Hodgkin's lymphoma on biopsy, in absence of other  $^{18}\text{F}$ -FDG-avid disease.

nign splenic lesions in either group of patients ( $P =$  not significant for all).

Twenty-one patients had  $>1$  splenic mass. Although all smaller lesions had lower SUVs in comparison with larger lesions in the same patients, only a weak correlation was found when comparing the SUV with the lesion size in the group as a whole ( $r = 0.65$ ,  $P < 0.001$ ).

## DISCUSSION

Splenic metastases are encountered in 2.3%–12.9% of postmortem examinations in cancer patients (20). The most common primary sites of malignancy to metastasize to the spleen are lung, breast, ovary, and melanoma (20,21). Splenic metastases are a relatively uncommon clinical event, usually occurring in the setting of disseminated metastatic disease (20,22), as was also seen in this study. To our knowledge, only 22 case reports of solitary splenic metastases are reported to date in the English literature, with more than one third of them secondary to lung cancer and malignant melanoma (23).

Although the spleen is a frequent site of involvement in patients with non-Hodgkin's lymphoma and may be in-

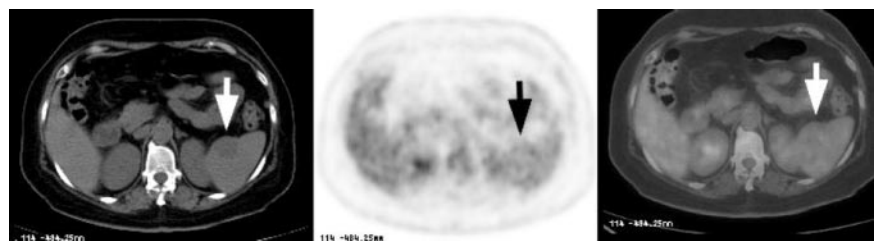
involved in one third of patients with Hodgkin's disease (24), primary malignant lymphoma of the spleen (PMLS) is uncommon. The definition of PMLS is controversial; however, it has been suggested that only cases with disease limited to the spleen and splenic hilum should be included in this entity (25). Although rare, PMLS is the most common primary malignancy of the spleen. Splenomegaly is not a reliable indicator of lymphomatous involvement of the spleen because the organ's size is normal in one third of patients with splenic disease (26). On imaging, lymphomatous involvement of the spleen may manifest as either focal lesions or diffuse disease. Recent reports have shown that  $^{18}\text{F}$ -FDG PET is more accurate than CT and gallium scintigraphy for identifying splenic involvement by lymphoma (27,28).

Primary nonhematopoietic tumors of the spleen are extremely rare. Tumors may arise from the sinus epithelium (angiosarcoma and hemangioendotheliomas) or from connective tissue (spindle cell sarcoma and fibrosarcoma). Of these rare entities, angiosarcoma is the most common tumor to involve the spleen with  $<100$  cases reported in the literature (29). Clinically, left upper quadrant abdominal pain, anemia, coagulopathy, and spontaneous rupture may be encountered. Hematogenous metastases at diagnosis are common and the overall prognosis is poor (30). Although there are no reports of  $^{18}\text{F}$ -FDG PET in the diagnosis of splenic angiosarcoma, angiosarcoma of the pleura and chest wall has been shown to be  $^{18}\text{F}$ -FDG avid (31).

As in the literature, the most common nonlymphomatous malignancies to metastasize to the spleen in our series were melanoma, lung, colon, and ovarian cancer. Although most patients with splenic metastases had disseminated metastatic disease, a few patients had disease limited to the spleen or the spleen and a solitary additional site, allowing a surgical approach to be considered as was the case in 2 of these patients in our series. In routine clinical practice, it is not possible to histologically confirm all sites of metastatic disease; therefore, we had to assume that an  $^{18}\text{F}$ -FDG-avid splenic lesion was a metastasis, based on positive histologic proof from another  $^{18}\text{F}$ -FDG-avid site and imaging follow-up of the splenic lesion.

Apart from accurate localization, one of the advantages of evaluation of lesions with PET/CT is the ability to evaluate non- $^{18}\text{F}$ -FDG-avid lesions, both visually and semiquantitatively, as accuracy of coregistration can be assessed. Known  $^{18}\text{F}$ -FDG-avid malignancies that had non- $^{18}\text{F}$ -FDG-avid

**FIGURE 3.** Presumably benign solid splenic mass: 62-y-old woman without previously diagnosed malignancy. Axial PET/CT images show no increased uptake of  $^{18}\text{F}$ -FDG within hypodense mass on CT (arrows). Mass was stable on sonography for  $>1$  year.



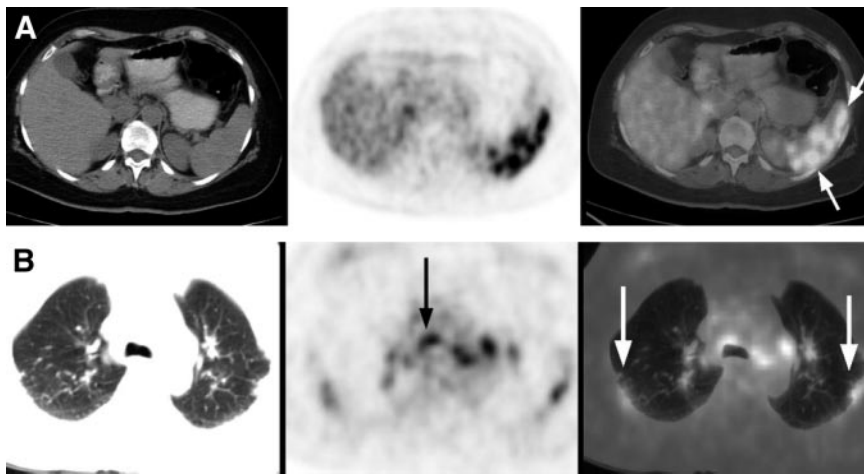


**FIGURE 4.** False-positive  $^{18}\text{F}$ -FDG PET/CT in sarcoidosis: 55-y-old woman without known malignancy. Multiple hypodense splenic nodules discovered on CT performed for abdominal pain. (A) Axial PET/CT images show innumerable  $^{18}\text{F}$ -FDG-avid nodules within spleen. (B) Axial PET/CT images (lung windows) show abnormal uptake of  $^{18}\text{F}$ -FDG in mediastinal lymph nodes (black arrow) as well as increased  $^{18}\text{F}$ -FDG uptake in subpleural lung densities (white arrows) proven to be sarcoidosis on lung biopsy.

splenic masses were all stable in size on follow-up of patients; although we do not have histologic diagnoses for most, these masses are presumed to be benign incidental masses. Splenic masses in patients with a known  $^{18}\text{F}$ -FDG-avid malignancy were accurately dichotomized by PET/CT assessment into benign or malignant. The sensitivity and specificity of visual PET reading for differentiating benign and malignant splenic lesions were 100% for patients with lymphoma or nonlymphomatous tumors. In this group of patients, using a SUV threshold of 2.3, all lesions would be correctly classified. However, it should be noted that there is a selection bias in this group of patients because it included patients that were sent for staging or restaging of primary malignancies that are considered  $^{18}\text{F}$ -FDG avid.

In the group of patients without a known malignancy,  $^{18}\text{F}$ -FDG PET had a high NPV. In fact, all lesions that did not show abnormal  $^{18}\text{F}$ -FDG uptake were stable on clinical and imaging follow-up and patients did not have evidence of malignancy during the follow-up time period (Fig. 3). Caution should be taken to avoid false-negative  $^{18}\text{F}$ -FDG PET results. Although no such cases were encountered in this study, it should be borne in mind that non- $^{18}\text{F}$ -FDG-avid tumors, such as some renal cell carcinomas or thyroid cancers, may metastasize to the spleen. In cases of non- $^{18}\text{F}$ -FDG-avid splenic lesions, the whole-body CT portion of the PET/CT studies should be thoroughly evaluated to assess for possible non- $^{18}\text{F}$ -FDG-avid malignancies. Using visual inspection and a SUV threshold of 2.2, false-positive  $^{18}\text{F}$ -FDG PET results were found in 2 patients. One of these patients had innumerable small foci of  $^{18}\text{F}$ -FDG uptake in the spleen as well as in subpleural lung densities and small mediastinal and hilar lymph nodes, a pattern suggestive of sarcoidosis (32), which was later verified on lung biopsy (Fig. 4). Because PET/CT studies combine both anatomic and functional imaging, patterns of disease on fused images may aid in suggesting a correct diagnosis. The second false-positive study was in a young woman with subcapsular  $^{18}\text{F}$ -FDG-avid masses shown on splenectomy to represent caseating granulomas due to *Brucella melitensis* (Fig. 5). Although

absent in this patient, abscesses due to *Brucella* described in the literature often show central calcific densities within the hypodense masses on CT (33). Similarly, it may be assumed that other granulomatous diseases involving the spleen, such as tuberculosis and histoplasmosis, as well as noninfectious inflammatory diseases, such as inflammatory pseudotumor, may abnormally accumulate  $^{18}\text{F}$ -FDG and imitate malignancy. A multiplicity of lesions, as expected, had a high PPV for malignancy (81.5%); however, granulomatous disease, which appears to be the most frequent etiology for false-positive  $^{18}\text{F}$ -FDG PET scans of the spleen, is not infrequently associated with multiple splenic lesions.

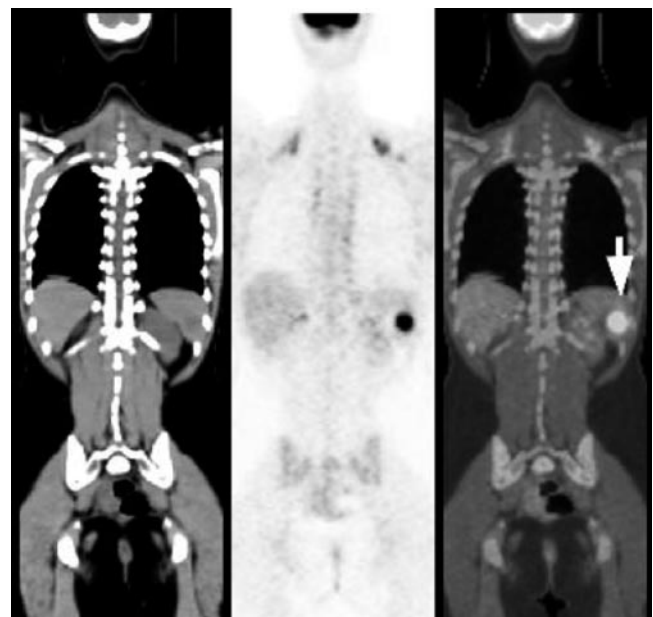


**FIGURE 5.** False-positive  $^{18}\text{F}$ -FDG PET/CT in splenic granulomas due to *Brucella melitensis*: 18-y-old woman with incidentally discovered solid splenic masses (arrow) on sonography performed because of epigastric pain. Coronal PET/CT images show abnormal uptake of  $^{18}\text{F}$ -FDG in splenic nodule, proven to be granuloma due to *Brucella* on splenectomy.

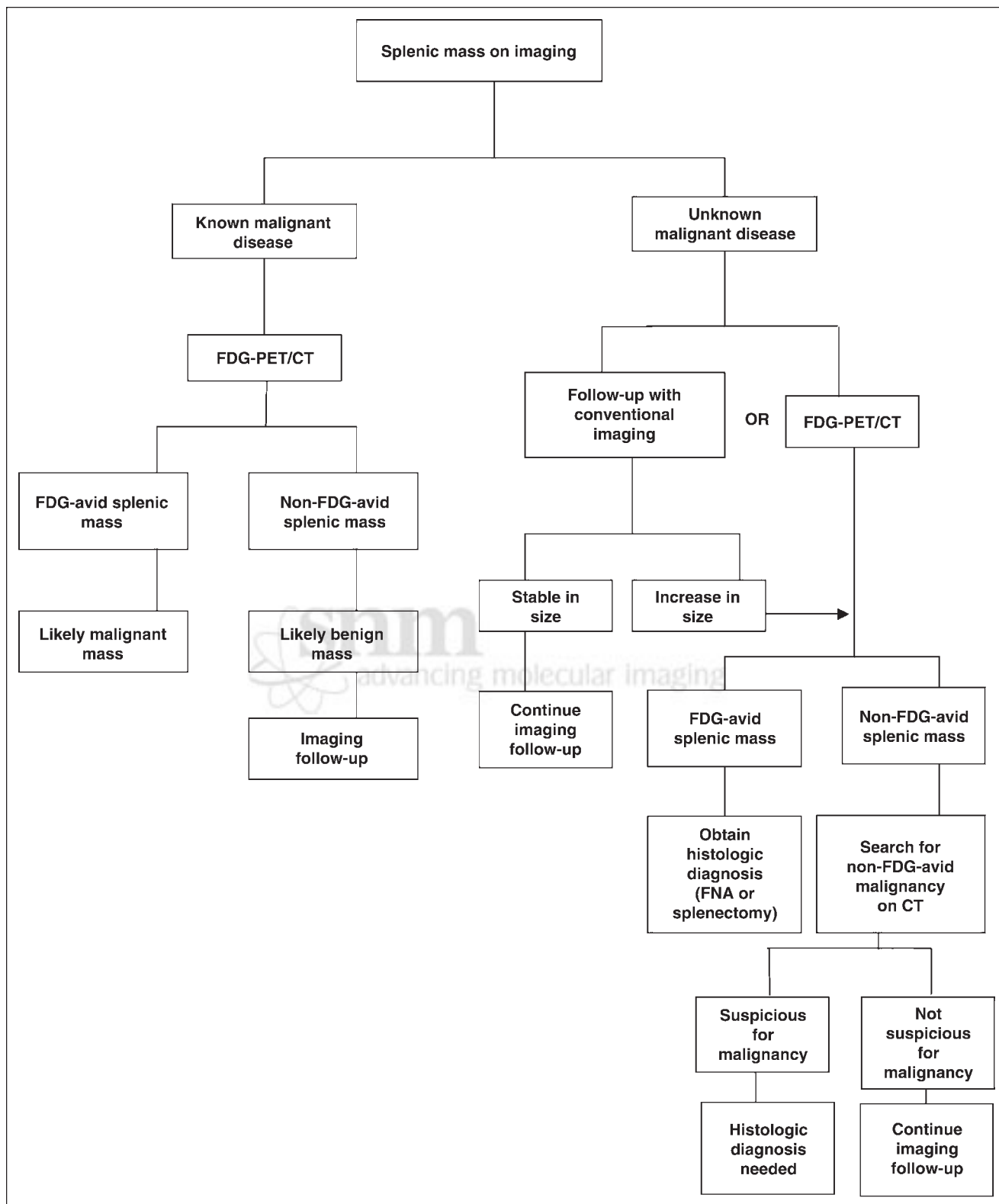


**FIGURE 6.** Suggested scheme for interpretation of a splenic lesion on PET/CT. FNA = fine-needle aspiration.

As previously shown for  $^{18}\text{F}$ -FDG PET of malignant lung nodules (34), smaller lesions in same patient had lower SUVs in comparison with larger lesions. A weak correlation between the SUV and the size of lesions in patients with >1

splenic mass as a group may be attributed to differences in uptake of  $^{18}\text{F}$ -FDG in the different primary tumors.

Because conventional imaging often cannot differentiate benign from malignant solid splenic masses, a new nonin-

vative imaging technique is needed. This study has shown that  $^{18}\text{F}$ -FDG PET/CT can be used to help discriminate benign from malignant splenic masses.  $^{18}\text{F}$ -FDG PET/CT can also identify additional unsuspected sites of disease, which may be more accessible for biopsy. This may obviate the need to biopsy the spleen itself, a procedure associated with a complication rate of 1.5%–13% (35,36). On the basis of this study's results, a possible scheme for interpretation of a splenic lesion on PET/CT is presented in Figure 6. This algorithm is suggested only if the primary tumor is  $^{18}\text{F}$ -FDG avid.

## CONCLUSION

$^{18}\text{F}$ -FDG PET can reliably discriminate between benign and malignant solid splenic masses in patients with known  $^{18}\text{F}$ -FDG-avid malignancy.  $^{18}\text{F}$ -FDG PET also appears to have a high NPV in patients with solid splenic masses, without known malignant disease.  $^{18}\text{F}$ -FDG-avid splenic masses in patients without a known malignancy should be further evaluated—in our series, 80% of them were malignant.

## ACKNOWLEDGMENT

The authors thank Israel Friedman for editorial assistance.

## REFERENCES

- Bragg DG, Colby TV, Ward JH. New concepts in the non-Hodgkin lymphoma: radiologic implications. *Radiology*. 1998;159:289–304.
- Castellino TA. Hodgkin disease: practical concepts for the diagnostic radiologist. *Radiology*. 1991;178:315–321.
- Paterson A, Frush DP, Donnelly LF, et al. A pattern-oriented approach to splenic imaging in infants and children. *Radiographics*. 1999;19:1465–1485.
- Lee SS, Morgenstern L, Phillips EH, Hiatt JR, Margulies DR. Splenectomy for splenic metastases: a changing clinical spectrum. *Am Surg*. 2000;66:837–840.
- Kutok JL, Fletcher CD. Splenic vascular tumors. *Semin Diagn Pathol*. 2003;20:128–139.
- Ramani M, Reinhold C, Semelka RC, et al. Splenic hemangiomas and hamartomas: MR imaging characteristics of 28 lesions. *Radiology*. 1997;202:166–172.
- Rabushka LS, Kawashima A, Fishman EK. Imaging of the spleen: CT with supplemental MR examination. *Radiographics*. 1994;14:307–332.
- Danon O, Duval-Arnould M, Osman Z, et al. Hepatic and splenic involvement in cat-scratch disease: imaging features. *Abdom Imaging*. 2000;25:182–183.
- Levy AD, Abbott RM, Abbondanzo SL. Littoral cell angioma of the spleen: CT features with clinicopathologic comparison. *Radiology*. 2004;230:485–490.
- Variami E, Terpos E, Vgenopoulou S, Kanellopoulou G, Meletis J. Inflammatory pseudotumor of the spleen: a case report and review of the literature. *Ann Hematol*. 1999;78:560–563.
- Terk MR, Esplin J, Lee K, et al. MR imaging of patients with type 1 Gaucher's disease: relationship between bone and visceral changes. *AJR*. 1995;165:599–604.
- Goerg C, Schwerek WB, Goerg K. Splenic lesions: sonographic patterns, follow-up, differential diagnosis. *Eur J Radiol*. 1991;13:59–66.
- Caslowitz PL, Labs JD, Fishman EK, Siegelman SS. Nontraumatic focal lesions of the spleen: assessment of imaging and clinical evaluation. *Comput Med Imaging Graph*. 1990;14:133–141.
- Moog F, Bangerter M, Diederichs CG, et al. Extranodal malignant lymphoma: detection with FDG PET versus CT. *Radiology*. 1998;206:475–481.
- Lardinois D, Weder W, Hany TF, et al. Staging of non-small-cell lung cancer with integrated positron-emission tomography and computed tomography. *N Engl J Med*. 2003;348:2500–2507.
- Schwimmer J, Essner R, Patel A, et al. A review of the literature for whole-body FDG PET in the management of patients with melanoma. *Q J Nucl Med*. 2000;44:153–167.
- Cohade C, Osman M, Leal J, Wahl RL. Direct comparison of  $^{18}\text{F}$ -FDG PET and PET/CT in patients with colorectal carcinoma. *J Nucl Med*. 2003;44:1797–1803.
- Pannu HK, Bristow RE, Cohade C, Fishman EK, Wahl RL. PET-CT in recurrent ovarian cancer: initial observations. *Radiographics*. 2004;24:209–223.
- Hany TF, Steinert HC, Goerres GW, Buck A, von-Schulthess GK. PET diagnostic accuracy: improvement with in-line PET-CT system—initial results. *Radiology*. 2002;225:575–581.
- Berge T. Splenic metastases: frequencies and patterns. *Acta Pathol Microbiol Scand*. 1974;82:499–506.
- Morgenstern L, Rosenberg J, Geller SA. Tumors of the spleen. *World J Surg*. 1985;9:468–476.
- Nathanson L, Hall TC, Farber S. Biological aspects of human malignant melanoma. *Cancer*. 1967;20:650–655.
- Hoar FJ, Chan SY, Stonelake PS, Wolverson RW, Bareford D. Splenic rupture as a consequence of dual malignant pathology: a case report. *J Clin Pathol*. 2003;56:709–710.
- Kadin ME, Glaststein EJ, Dorfman RE. Clinicopathologic studies in 117 untreated patients subject to laparotomy for the staging of Hodgkin's disease. *Cancer*. 1977;27:1277–1294.
- Brox A, Shustik C. Non-Hodgkin's lymphoma of the spleen. *Leuk Lymphoma*. 1993;11:165–171.
- Castellino RA, Marglin S, Blank N. Hodgkin's disease, the non-Hodgkin's lymphomas and the leukemias in the retroperitoneum. *Semin Roentgenol*. 1980;15:288–301.
- Rini JN, Leonidas JC, Tomas MB, Palestro CJ.  $^{18}\text{F}$ -FDG PET versus CT for evaluating the spleen during initial staging of lymphoma. *J Nucl Med*. 2003;44:1072–1074.
- Kostakoglu L, Leonard JP, Kuji I, et al. Comparison of fluorine-18 fluorodeoxyglucose positron emission tomography and Ga-67 scintigraphy in evaluation of lymphoma. *Cancer*. 2002;94:879–888.
- Smith VC, Eisenberg BL, McDonald EC. Primary splenic angiosarcoma: case report and literature review. *Cancer*. 1985;55:1625–1627.
- Autry JR, Weitzner S. Hemangiosarcoma of spleen with spontaneous rupture. *Cancer*. 1975;35:534–539.
- Del Frate C, Morte K, Zanardi R, et al. Pseudomesotheliomatous angiosarcoma of the chest wall and pleura. *J Thorac Imaging*. 2003;18:200–203.
- Warshauer DM, Lee JK. Imaging manifestations of abdominal sarcoidosis. *AJR*. 2004;182:15–28.
- Ariza J, Pigrau C, Canas C, et al. Current understanding and management of chronic hepatosplenic suppurative brucellosis. *Clin Infect Dis*. 2001;32:1024–1033.
- Hara T, Kosaka N, Suzuki T, et al. Uptake rates of  $^{18}\text{F}$ -fluorodeoxyglucose and  $^{11}\text{C}$ -choline in lung cancer and pulmonary tuberculosis: a positron emission tomography study. *Chest*. 2003;124:893–901.
- Lindgren PG, Hagberg H, Eriksson B, et al. Excision biopsy of the spleen by ultrasound guidance. *Br J Radiol*. 1985;58:853–857.
- Keogan MT, Freed KS, Paulson EK, et al. Imaging-guided percutaneous biopsy of focal splenic lesions: update on safety and effectiveness. *AJR*. 1999;172:933–937.



The Journal of  
NUCLEAR MEDICINE

## Solid Splenic Masses: Evaluation with $^{18}\text{F}$ -FDG PET/CT

Ur Metser, Elka Miller, Ada Kessler, Hedva Lerman, Gennady Lievshitz, Ran Oren and Einat Even-Sapir

*J Nucl Med.* 2005;46:52-59.

---

This article and updated information are available at:  
<http://jnm.snmjournals.org/content/46/1/52>

---

Information about reproducing figures, tables, or other portions of this article can be found online at:  
<http://jnm.snmjournals.org/site/misc/permission.xhtml>

Information about subscriptions to JNM can be found at:  
<http://jnm.snmjournals.org/site/subscriptions/online.xhtml>

*The Journal of Nuclear Medicine* is published monthly.  
SNMMI | Society of Nuclear Medicine and Molecular Imaging  
1850 Samuel Morse Drive, Reston, VA 20190.  
(Print ISSN: 0161-5505, Online ISSN: 2159-662X)

© Copyright 2005 SNMMI; all rights reserved.